

Research Article

Analysis of Thermal Comfort in a Residential Room with Multiple Vents: A Case Study by Numerical Simulation Technique

¹D. Prakash and ²P. Ravikumar

¹Department of Mechanical Engineering, Anna University, Trichy, India

²Department of Mechanical Engineering, St. Joseph College of
Engineering and Technology, Thanjavur, India

Abstract: Thermal comfort is very essential for the occupants in the residential building without air-conditioning system in the hot and arid climatic regions. In this study, the thermal comfort prevailed inside the room with window openings at their adjacent walls was analyzed under various wind directions by computational fluid dynamic technique. The CFD simulation was validated with the experimental results obtained from wind tunnel test rig and network model and found that it is having a good agreement. The room with single window opening at the adjacent walls was investigated under various wind directions and based on their prevailed uncomforted zones, the window opening at the windward side wall was split in to multiple vents as double and triple vent system without changing window opening area. From this study, it was identified that the triple vent system reduces the indoor temperature and predicted mean vote by 0.3 and provides improved uniform thermal comfort.

Keywords: Computational fluid dynamics, multiple vent system, natural ventilation, predicted mean vote, thermal comfort

INTRODUCTION

Thermal comfort is the state of mind that expresses satisfaction to the occupants with the thermal environment. Thermal comfort can be enhanced by providing good indoor air ventilation through natural means and mechanical systems. Even though the mechanical ventilation is having high capability to control the indoor space at the required temperature, it was prone to the cause of sick building syndrome and building related sickness. The thermal comfort survey conducted in Bangkok by Busch (1992) suggests that people can tolerate even higher temperature in naturally ventilated buildings than in mechanically ventilated buildings. Also many mechanical ventilation systems do not deliver the desired air quality and it is the source for indoor contaminants that would contribute building related health symptom (Godish and Spengler, 1996). Hence, the natural ventilation is a promising solution for providing good thermal comfort.

For a naturally ventilated building, it is essential to predict thermal comfort through thermal comfort index, since other parameters like ventilation rate and air change hour cannot predict the level of comfort with in the space. Fanger's developed the thermal comfort model-Predicted Mean Vote (PMV) which includes three personal parameters namely metabolism, work

and thermal resistance of clothing and four environmental factors as air temperature, radiant temperature, air velocity and water vapour pressure in the air. Mean while, most of the research works on building ventilation pertains to single sided ventilation (Marcello *et al.*, 2011; Larsen and Heiselber, 2008; Zhen and Shinsuke, 2011) and cross ventilation (windows located at the opposite sides of the wall) (Evalo and Popov, 2006; Visagavel and Srinivasan, 2009). But in the real case, the window openings are located at the adjacent sides of the room walls.

In this context present work is focused to study the thermal comfort in a residential room with window openings at the adjacent wall. The importance of choosing such a window orientation in building ventilation was discussed by Ravikumar and Prakash (2009, 2011).

This study also includes the analysis on modified form of traditional window opening that provides uniform indoor thermal comfort under wide range of wind incidence direction. In the present study, the air flow inside the building was investigated by Computational Fluid Dynamic technique (CFD). Xiong *et al.* (2012) and Ramponi and Blocken (2012) performed the air flow analysis in the buildings by using CFD due to its informative results and low labor and equipment costs.

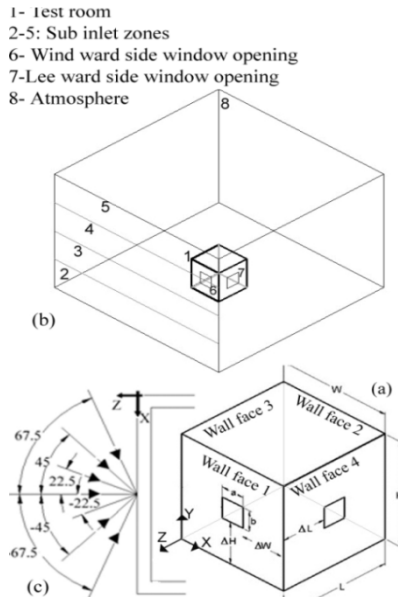


Fig. 1: (a) Test case room (b) CFD model (C) analyzed wind direction representation

TEST CASE ROOM AND CFD METHODOLOGY

A typical room of size 5×5×4 m (L×W×H) with two window openings of size 1×1 m on the adjacent side walls are modelled. This room model was placed inside a three dimensional box of size 30×30×20 m. The 3-D box was considered as an external atmospheric zone around the room model. The CFD model was created in the GAMBIT software and was shown in Fig. 1.

Governing equation of fluid flow: The fundamental equations which govern the fluid flow are conservation of mass, momentum equation and conservation of energy.

Conservation of mass: Conservation of mass states that the rate of increase in the density, ρ in a control volume dx, dy, dz should be equal to the net rate of influx of mass to the control volume:

$$\frac{\partial \rho}{\partial t} + \frac{\partial (\rho v_x)}{\partial x} + \frac{\partial (\rho v_y)}{\partial y} + \frac{\partial (\rho v_z)}{\partial z} = 0 \quad (1)$$

Conservation of momentum: Conservation of momentum states that the net force on the control volume in any direction equals the efflux of momentum minus the influx of momentum in the same direction.
x direction:

$$\frac{\partial \rho v_x}{\partial t} + \frac{\partial (\rho v_x v_x)}{\partial x} + \frac{\partial (\rho v_x v_y)}{\partial y} + \frac{\partial (\rho v_x v_z)}{\partial z} = \rho g_x - \frac{\partial P}{\partial x} + R_x + \frac{\partial}{\partial x} \left(\mu_e \frac{\partial v_x}{\partial x} \right) + \frac{\partial}{\partial y} \left(\mu_e \frac{\partial v_x}{\partial y} \right) + \frac{\partial}{\partial z} \left(\mu_e \frac{\partial v_x}{\partial z} \right) + \tau_x \quad (2)$$

y direction:

$$\frac{\partial \rho v_y}{\partial t} + \frac{\partial (\rho v_x v_y)}{\partial x} + \frac{\partial (\rho v_y v_y)}{\partial y} + \frac{\partial (\rho v_y v_z)}{\partial z} = \rho g_y - \frac{\partial P}{\partial y} + R_y + \frac{\partial}{\partial x} \left(\mu_e \frac{\partial v_y}{\partial x} \right) + \frac{\partial}{\partial y} \left(\mu_e \frac{\partial v_y}{\partial y} \right) + \frac{\partial}{\partial z} \left(\mu_e \frac{\partial v_y}{\partial z} \right) + \tau_y \quad (3)$$

z direction:

$$\frac{\partial \rho v_z}{\partial t} + \frac{\partial (\rho v_x v_z)}{\partial x} + \frac{\partial (\rho v_y v_z)}{\partial y} + \frac{\partial (\rho v_z v_z)}{\partial z} = \rho g_z - \frac{\partial P}{\partial z} + R_z + \frac{\partial}{\partial x} \left(\mu_e \frac{\partial v_z}{\partial x} \right) + \frac{\partial}{\partial y} \left(\mu_e \frac{\partial v_z}{\partial y} \right) + \frac{\partial}{\partial z} \left(\mu_e \frac{\partial v_z}{\partial z} \right) + \tau_z$$

where,

- v_x, v_y & v_z : The components of velocity in x, y and z directions
- ρ : The density
- t : The time
- g : The gravity
- μ_e : The effective viscosity
- P : The pressure
- R_i : The distributed resistance
- Suffix i : x, y and z
- τ : The viscous loss

Conservation of energy: Conservation of energy in the control volume dx, dy, dz states that the net increase in internal energy in the control volume equals the net flow of energy by convection plus the net inflow by thermal and mass diffusion:

$$\frac{\partial}{\partial t} (\rho C_p T_o) + \frac{\partial}{\partial x} (\rho v_x C_p T_o) + \frac{\partial}{\partial y} (\rho v_y C_p T_o) + \frac{\partial}{\partial z} (\rho v_z C_p T_o) = \frac{\partial}{\partial x} \left(K \frac{\partial T_o}{\partial x} \right) + \frac{\partial}{\partial y} \left(K \frac{\partial T_o}{\partial y} \right) + \frac{\partial}{\partial z} \left(K \frac{\partial T_o}{\partial z} \right) + W^v + E_k + Q_v + \phi + \frac{\partial P}{\partial t} \quad (5)$$

where,

- C_p = The specific heat
- T_o = The total temperature
- K = The thermal conductivity
- W^v = The viscous work term
- Q_v = The volumetric heat source
- ϕ = The viscous heat generation term
- E_k = The kinetic energy

Standard k-ε model: The standard k-ε model is a semi empirical model based on turbulent kinetic energy (k) and dissipation rate (ε). In the derivation of k- ε model, the flow was assumed to be fully turbulent and the effect of molecular viscosity is negligible. The turbulence kinetic energy and its rate of dissipation are obtained from the following transport equations:

$$\frac{\partial}{\partial t} (\rho k) + \frac{\partial}{\partial x_j} (\rho k u_j) = \frac{\partial}{\partial x_j} \left[\left(\mu + \frac{\mu_t}{\sigma_k} \right) \frac{\partial k}{\partial x_j} \right] + G_k + G_b - \rho \epsilon - Y_M + S_k \quad (6)$$

$$\frac{\partial}{\partial t}(\rho\varepsilon) + \frac{\partial}{\partial x_i}(\rho\varepsilon u_i) = \frac{\partial}{\partial x_j} \left[\left(\mu + \frac{\mu_t}{\sigma_\varepsilon} \right) \frac{\partial \varepsilon}{\partial x_j} \right] + C_{1\varepsilon} + (G_k + C_{3\varepsilon}G_b) - C_{2\varepsilon}\rho \frac{\varepsilon^2}{k} + S_\varepsilon \quad (7)$$

The turbulent viscosity μ_t is predicted from k and ε forms the following equation:

$$\mu_k = \rho C_\mu \frac{k^2}{\varepsilon} \quad (8)$$

In the above equation,

G_k : The generation of turbulence kinetic energy due to mean velocity gradients

G_b : The generation of turbulence kinetic energy due to buoyancy

Y_M : The contribution of fluctuation dilatation in compressible turbulence to the overall dissipation rate

The model constants $C_{1\varepsilon} = 1.44$, $C_{2\varepsilon} = 1.92$, $C_\mu = 0.09$, $\sigma_k = 1.0$, $\sigma_\varepsilon = 1.3$. These constants have been determined from experiments with air and water for fundamental turbulent shear flows including homogeneous shear flows and decaying isotropic grid turbulence. The standard k - ε model is the most commonly used and validated turbulence model in engineering applications. The popularity of this model is due to its robustness in a wide range of industrially relevant flows low computational costs and generally better numerical stability than more complex turbulence models (Versteeg and Malalasekara, 1995).

Assumptions: The major assumptions involved in the present research of CFD analysis in building ventilation are as follows:

- Ventilation due to wind force was only considered.
- An isolated room was analyzed.
- Air properties are assumed as a constant value with reference to atmospheric temperature.
- Building materials thermal properties are constant with reference to the atmospheric temperature.

Boundary conditions: The following boundary conditions are applied to the flow domain:

At the inlet of the atmospheric zone, the wind velocity was specified. In general, velocity of air flow varies with respect to building height. This variation was specified either by logarithmic profile (Evalo and Popov, 2006) or by dividing the velocity inlet into may sub inlet zones (Asfour and Gadi, 2007). In this study, the wind entering zone is divided in to 4 sub inlet zones. The wind velocity at these sub zones are predicted from the Eq. (9) (Asfour and Gadi, 2007):

$$V = V_r cH^a \quad (9)$$

where,

V = The wind speed from the ground level (m/s).

V_r = The reference wind speed measured experimentally

H = The height at which Velocity (V) was predicted

c = The parameter relating wind speed to terrain nature (0.68 in the open country terrain)

a = The exponent relating wind speed to the height above the ground (0.17 in the open county terrain)

The boundary conditions applied to this CFD simulation are measured for an existing building on one summer day at noon time. The measured values of temperature for various zones are as follows. Roof temperature 325 K, Room side walls -312 K; Floor temperature 303 K; Ambient temperature 306 K and Wind velocity 1 m/s. Also Free slip boundary conditions were employed to the room wall, roof and floor surfaces. The analysed room was assumed to have some electrical appliances and two human beings. The heat generated from the electrical appliances and human beings are assumed 25 w/m².

The tetrahedral hybrid T grid type element of size 0.5 m is used for meshing the flow domain. This grid size was independent to the results as verified by repeating the test with a greater number of cells. Standard k- ε turbulence model was employed. The fluid model shown in Fig. 1b was solved in FLUENT 6.1 software by segregated solver. Second order upwind method was used to iterate up to a convergence level of 10⁻⁶ for all flow variables.

Validation of CFD simulation: The purpose of validation is to check the accuracy of CFD code so that CFD code may be used with confident in the simulation of airflow studies. Hence in this research work a detailed validation of CFD simulation was conducted through wind tunnel test rig and Network model.

Validation of CFD simulation with wind tunnel test rig: A reduced scale model of the cube which refers to the room was made and placed in the subsonic wind tunnel shown in Fig. 2.

In the wind tunnel, the contraction cone take a large volume of low velocity air and reduce it to small volume of high velocity air. The shape of the contraction cone was a cubic curve and next to contraction cone, settling chamber was provided. The settling chamber straightens the air flow as the wind tunnel draws air in from the surrounding air. In the straightening chamber a series of honey comb tubes are provided in order to make the airflow parallel. The model was scaled down by 1:35 and holes were provided along the cube surface for measuring the pressure. Surface pressure was measured at 12 locations on the vertical façade and 7 locations at the roof surface. The measurements were performed with the Pitot tube manometer. Small tubes of diameter 3 mm are inserted in the holes of the test cube. Other end of

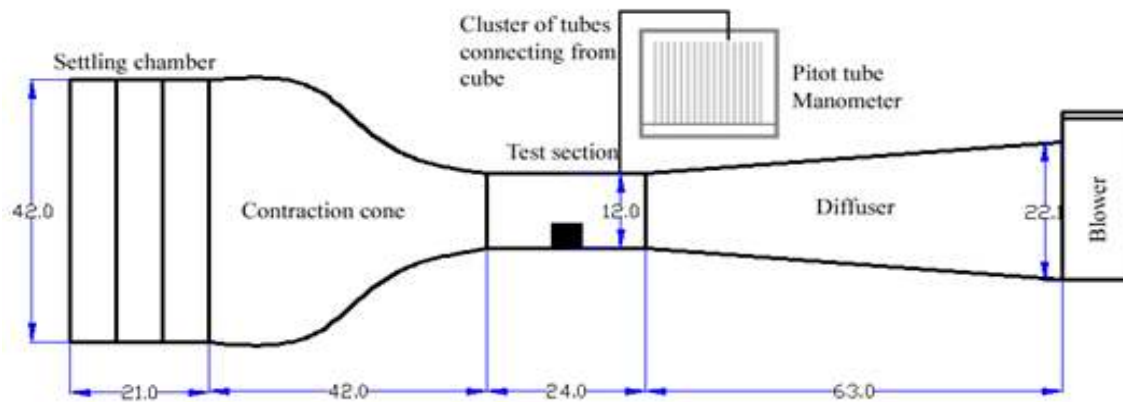


Fig. 2: Wind tunnel test rig-schematic layout

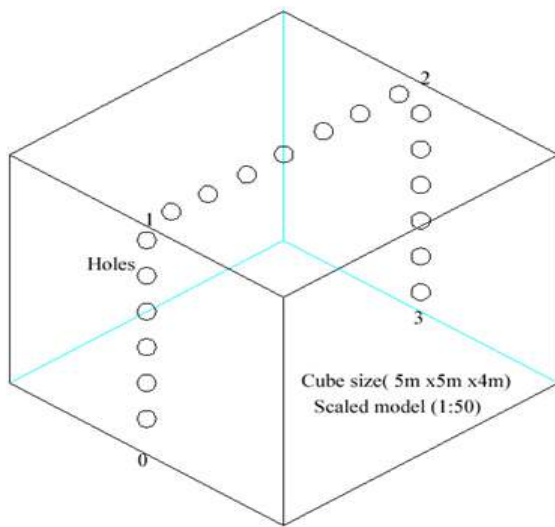


Fig. 3: Scaled room model tested in wind tunnel test rig

the tubes are connected the Pitot tube manometer. The reduced scale model made for this study was shown in Fig. 3.

For the tested cube, the pressure coefficients along the cube surface are predicted from the Eq. (10):

$$C_p = \frac{P - P_o}{(0.5 \times \rho \times v^2)} \quad (10)$$

where,

P = The static pressure at the tested location

P_o = Free stream static pressure

ρ = Free stream density

v = Free stream velocity

The CFD simulation for the flow over the cube was performed and the pressure coefficients along the same cube surface were predicted and their comparison with the pressure coefficient determined from the scaled model at wind tunnel test rig was shown in Fig. 4.

In this figure, the CFD predicted pressure coefficient values along the cube surface have the similar trend as experimental values for the scaled model. However, the CFD predicted C_p values are having some deviation at the wind ward side and having comparatively good agreement on the roof and leeward side. By considering this deviation as a negligible level, the CFD simulation was validated with the experimental testing of cube surface in the wind tunnel test rig.

Validation of CFD simulation with network model:

The CFD simulation of air flow over the cube surface was validated with the experimental testing of scaled model and discussed in the previous section. In this section, the same cubic model with openings is compared with the Network model. This comparison adds the validation of CFD simulation. In this validation process, the mass flow rate of air passing through the window openings was determined from the CFD simulation and it was compared with the mass flow rate predicted from the Network model. This method could be useful for studies that have no access to laboratory or full-scale testing facilities. The airflow rate induced by the wind pressure difference was calculated from the equation:

$$Q_{network} = A_{Effective} \sqrt{\left(\frac{2\Delta p}{\rho}\right)} \quad (11)$$

where,

$Q_{network}$ = Airflow rate through the window opening (m^3/s)

$A_{effective}$ = Effective area of opening (m^2)

Δp = Pressure difference across the window opening (Pa)

ρ = Air density (kg/m^3)

The pressure difference across the window opening can be calculated from the Eq. (12):

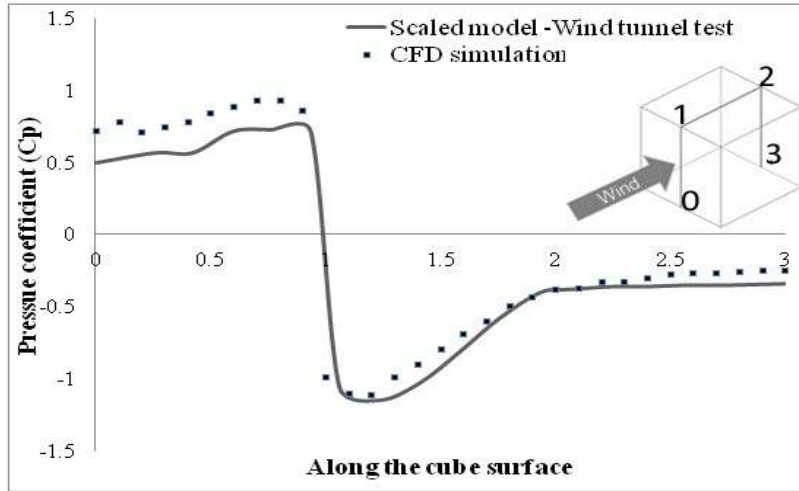


Fig. 4: Comparison of pressure coefficient predicted from CFD simulation and wind tunnel test

Table 1: Discrepancy of CFD simulation with network model

Mass flow rate (kg/s)		CFD prediction			Discrepancy (%)		
Wind angle (°)	Network model	Single vent	Double vent	Triple vent	Single vent	Double vent	Triple vent
-45	0.61	0.58	0.56	0.57	4.9	8.2	6.5
-22.5	0.70	0.68	0.67	0.68	3.5	4.2	2.8
0	0.77	0.76	0.75	0.77	1.5	3.1	1.0
22.5	0.70	0.69	0.68	0.68	1.8	2.8	2.5
45	0.61	0.58	0.55	0.58	5.2	9.5	4.9

$$\Delta p = 0.5 \rho V^2 \left| C_{pn} - C_{pi} \right| \quad (12)$$

where,

V = The wind velocity at the datum level (m/s)

C_{pn} = The pressure coefficient at nth opening

C_{pi} = The internal pressure coefficient

Substituting the Eq. (12) in (11) then:

$$Q_{network} = A_{effective} V (C_{pn} - C_{pi}) (C_{pn} - C_{pi})^{-1/2} \quad (13)$$

By considering the Law of conservation of mass the above equation can be rewritten as:

$$\sum_{n=1}^N A_{effective} V (C_{pn} - C_{pi}) (C_{pn} - C_{pi})^{-1/2} = 0 \quad (14)$$

From the above equation it is possible to estimate the internal pressure coefficient by knowing the C_{pn} value.

The C_{pi} is determined from the law of conservation and is given in the Eq. (14) (Asfour and Gadi, 2007):

$$\left| C_{pn} - C_{pi} \right|^{-0.5} + \left| C_{p(n+1)} - C_{pi} \right|^{-0.5} = 0 \quad (15)$$

This method of validation was performed for all the cases analyzed in this research work. The mass flow rate predicted from the CFD simulation and Network model for this study and its discrepancy values for all the cases are presented in Table 1.

From the above table, the discrepancy value of mass flow rate predicted from CFD simulation with network model is not significant and hence the CFD simulation is having good agreement with Network model also. This method could be useful for studies that have no access to laboratory or full-scale testing facilities. Such a method of validation was implemented by Asfour and Gadi (2007) also for the room with cross ventilation.

AIRFLOW CHARACTERISTICS FOR MULTIPLE VENT SYSTEM

In the first modification, the single vent was splitted in to two vents and in the second modification it was splitted in to three vents as shown in Fig. 5. In both modifications, the total area of the window open was kept as 1 m².

The temperature trends along the midline X1X2, Y1Y2 and Z1Z2 are shown in Fig. 6.

In the X1X2 midline the temperature trend for the single vent case for all the wind directions is not

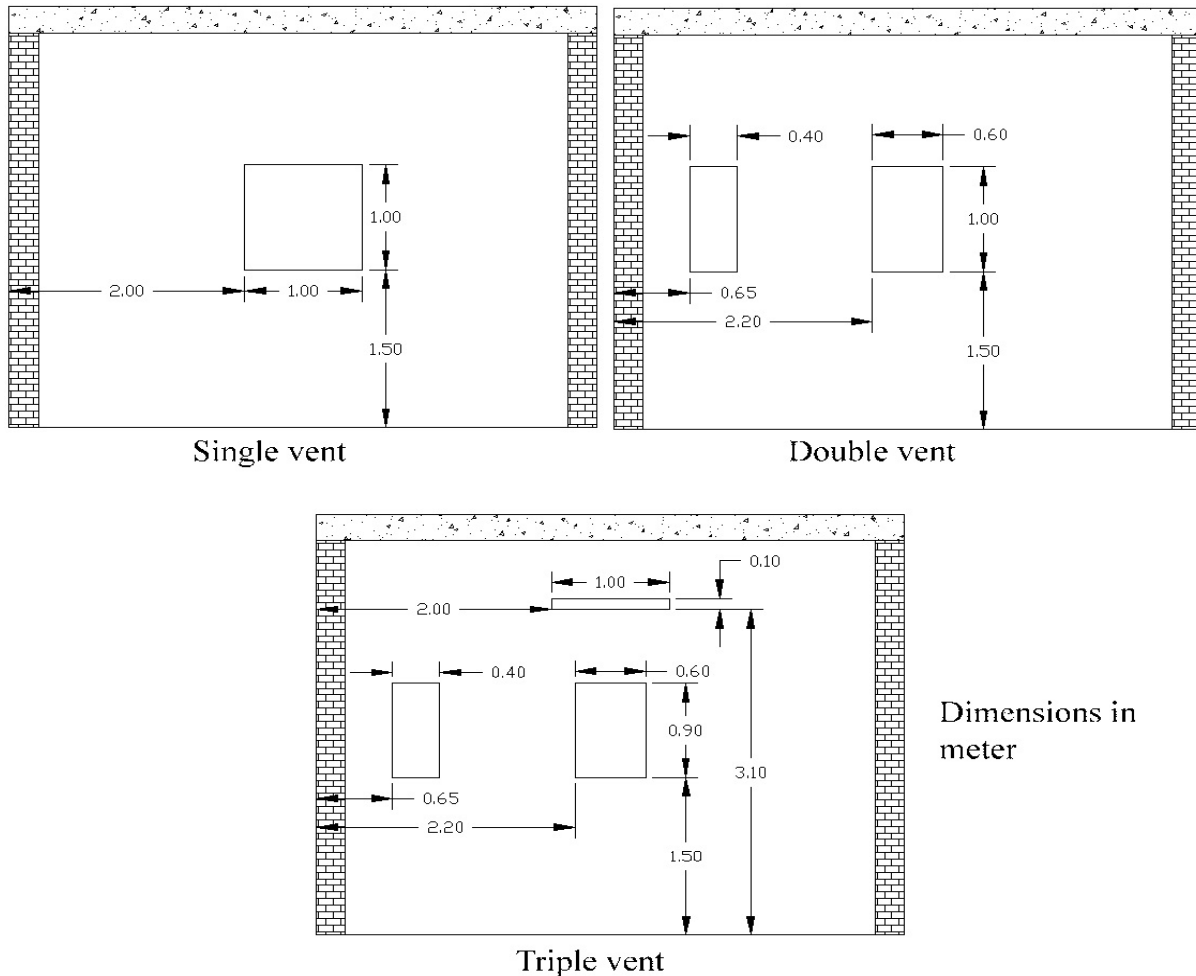


Fig. 5: Modification of single vent system as multiple vent-layout

uniform. Except for $\alpha = 45^\circ$ all the wind directions are having elevated temperature from $x = 2^{\text{nd}}$ m towards the wall face 3. This variation in temperature is about 1.5°C . From the 2^{nd} to 4^{th} m, the temperature is almost constant for all the wind directions. It is evident that the temperature from $x = 0^{\text{th}}$ to 2^{nd} m in the X1X2 midline is having high temperature and hence a secondary opening is required in between this distance. Hence, the single window open of size (1×1) m is splitted in to two vents. The second vent was positioned at a distance of 0.65 m in the X direction and 1.5 m from the ground surface. The double vent drastically reduces the temperature along the X1X2 midline in comparison with single vent.

In the double vent system, upto 1 m, the temperature was constant and between 1 to 2 m the temperature was decreasing and again from 3^{rd} to 4^{th} m the temperature was increased slightly. However, all the wind directions provide almost similar type of temperature trend. Further more, in triple vent system, the temperature trend along the midline X1X2 is not having much variations in comparison with double vent.

But, a slight decrease in the temperature was identified along the X1X2 for all the wind directions in triple vent system. The temperature trend along the midline Y1Y2 are also shown in Fig. 6. For the single vent case, the temperature increases from the ground surface to $y = 1.5^{\text{th}}$ m height, and decreases from 1.5^{th} m to $y = 3^{\text{rd}}$ m and again increases rapidly from 3^{rd} m to the roof surface. This variation in temperature along Y1Y2 in increasing linearly from wind direction $\alpha = 45^\circ$ to $\alpha = 45^\circ$. But in the double vent case, the temperature is increasing marginally upto a height of 1 m and from 1^{st} to 2^{nd} m it is almost constant and above 2 m, the temperature was increasing drastically upto the roof surface. However, the temperature rise from 2^{nd} m to roof surface is higher for double vent system than single vent system. This trend was noticed for all the wind directions, since the single vent was splitted into two vents, the entrapped wind force is not enough to travel upto a height of 4 m from the ground surface. But this double vent reduces the temperature for about 0.5°C upto a height of 2 m in comparison with single vent.

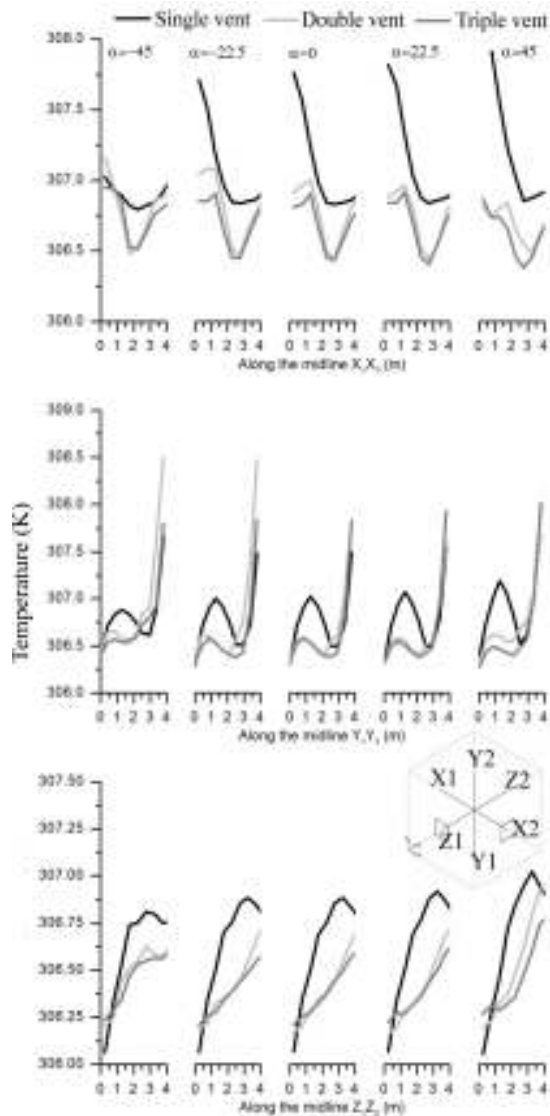


Fig. 6: Temperature variation along the midlines X1X2, Y1Y2 and Z1Z2

Hence, the double vent was further modified to triple vent system. In the triple vent system, the height of the second vent system was reduced to 0.9 m and a third vent of size 1×0.1 m was introduced centrally in the windward side wall at a height of 3.1 m from the ground surface. In the triple vent system, the temperature is almost constant at about 306.5 K upto a height of 3rd m for the wind direction $\alpha = 45^\circ$. For other wind directions, the temperature is increasing slightly upto 1 m and decreasing upto 3rd m and again increasing upto roof surface. But this variation and temperature magnitude is comparatively lower than single and double vent system. The temperature trend along Z1Z2 is also shown in the Fig. 6. For other wind directions, the temperature is increasing slightly upto 1m and decreasing upto 3rd m and again increasing upto roof surface. But this variation

and temperature magnitude is comparatively lower than single and double vent system. The temperature trend along Z1Z2 is also shown in the figure 6. For the wind direction $\alpha = 45^\circ$ the temperature for single vent systems is increasing upto a distance of 1.5 m in Z1Z2 midline and after that the temperature is almost constant. While the other wind directions have the increase in temperature upto 3rd m and later a slight fall in temperature was identified. The temperature for single vent system in the Z1Z2 midline varies from 306 to 307 K. The double vent system reduces this temperature drastically for all the wind directions except $\alpha = 45^\circ$. For the wind directions $\alpha = 45^\circ$ to 22.5° , the temperature along Z1Z2 is very low in comparison with single vent system and the temperature variation is in the range of 306.25 to 306.75 K. In the second modification-triple vent system further reduction in temperature magnitude was noticed along the Z1Z2 midline. For all the wind directions, similar pattern of temperature trend in the Z1Z2 midline was identified with a maximum temperature rise of 0.5°C. With all these trends, triple vent system was identified as the best vent window pattern at the windward side wall for the room with windows at their adjacent walls. The velocity vector plot and temperature plot for single, double and triple vent system for the wind direction of $\alpha = 0^\circ$ at the plane of 2 m from ground surface was shown in (Fig. 7).

For the single vent system, the air enters through the windward side wall and leaves the leeward side wall with a recirculation zone at the top right corner. Also there is no air flow near the wall face 3. In the double vent system, the air is allowed to enter through two vents which causes the air to travel along the wall face 3 also. In the triple vent system, the flow pattern of air is very much similar to double vent system and high impact of inlet air on the wall face 2 was reduced. The temperature pattern is also shown in the same Fig. 7. In the single vent system the temperature near the wall face 3 is comparatively high. This is due to the poor air circulation at this zone and hence the modified system of double vent was introduced. The temperature plot for the double vent case shows uniform temperature with the variation of the 0.4°C. However the variation of temperature in the single vent system was about 2°C. Also in the double vent system the temperature of indoor air temperature was reduced at all the locations in comparison with single vent system. The triple vent system also shows similar pattern of temperature as in double vent system. From the Fig. 7, it was clearly evident that triple vent system is the best window pattern to provide uniform and low indoor temperature. However, to quantify the performance of analyzed vent systems, another parameter "low temperature zone" was predicted in this study. Low temperature zone is the zone having temperature in the range of 306 to 307 K.

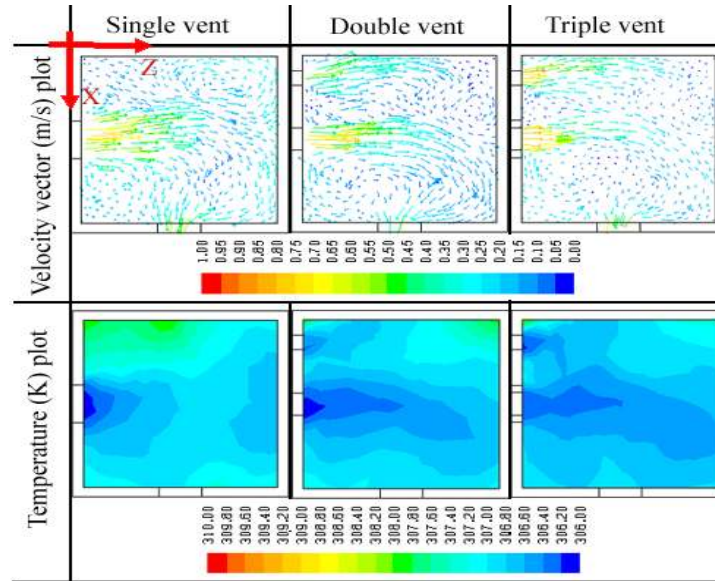


Fig. 7: Velocity and temperature plot at the plane parallel to ground surface at a height of 2 m

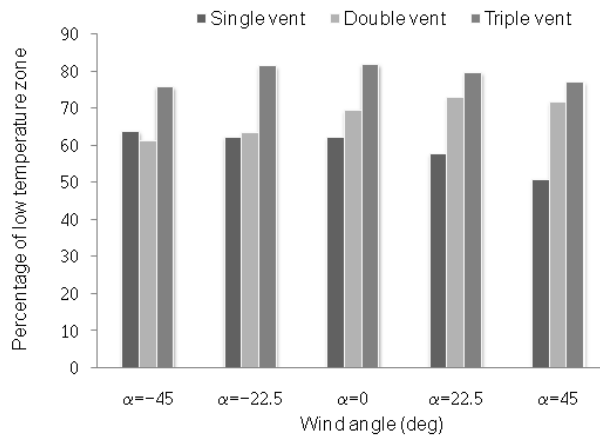


Fig. 8: Average percentage of low temperature zone for multiple vent system

This low temperature zone was predicted for the three vent systems under the wind directions $\alpha = -45^\circ$ to 45° and an average percentage of low temperature zone was predicted. The average percentage of low temperature zone obtained for the single vent and modified vent systems are predicted and shown in Fig. 8.

Single vent system yields about 60% of low temperature zone for all the wind directions. This percentage of low temperature zone is maximum for $\alpha = -45^\circ$ and reducing gradually towards $\alpha = 45^\circ$. In the double vent system for the wind angle $\alpha = 45^\circ$ and -22.5° the percentage of low temperature zone was slightly reduced in comparison with single vent system. This is due to splitting of single vent into double vent and in turn it locally rises the temperature at the height of 3m from the ground surface. But for other wind directions like $\alpha = 0^\circ$, 22.5° and 45° , this percentage of low temperature zone was improved gradually. In the

triple vent system, the percentage of low temperature zone was improved drastically in comparison with other two vent systems. About 80% of the room interior was provided with low temperature zone under all the wind directions. Thus triple vent system improved the low temperature zone by 20% in comparison with single vent system which is the conventional window pattern. Hence it is good to split the window system into three vents as prescribed for providing good indoor comfort. This three vent system controls and allows the air to travel the entire zone of the room interior and thereby the entrapped air was effectively utilized for indoor heat removal.

THERMAL COMFORT INDEX

Fanger's (Awbi, 2003) thermal comfort model-Predicted Mean Vote (PMV) based on a physical

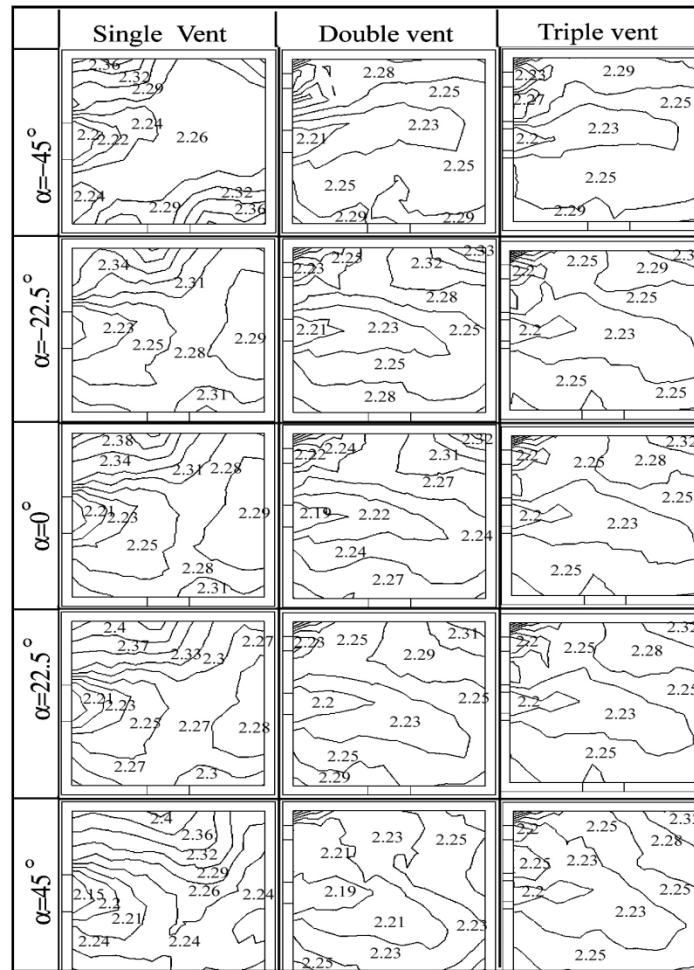


Fig. 9: PMV contour for the plane parallel to ground surface at a height of 2 m

assessment of heat exchange between the human body and the environment was used in this study to predict the thermal comfort given in Eq. (16). The PMV value has a range of +3.0 to -3.0, corresponding with the hot and cold thermal conditions. For the determination of PMV value, the metabolic rate, work completed and thermal resistance of clothing are assumed as 70 W/m^2 , 30 W and $0.11 \text{ (m}^2/\text{k) /W}$, respectively (Awbi, 2003).

Figure 9 shows the PMV contour plot predicted at plane parallel to the ground at the height of 2 m.

In the single vent system, the PMV value is lower for the wind directions $\alpha = -45^\circ$ and -22.5° in comparison with other wind directions. For the wind direction $\alpha = -45^\circ$ the central portion is having the PMV value of 2.26 and for $\alpha = -22.5^\circ$ the PMV value is 2.28. For $\alpha = -22.5^\circ$ a small portion nearer to the wall face 2 is experiencing a high PMV value of 2.29. This shows that the entrapped air is not travelling in to this zone and hence the temperature at this region is increased slightly. Also the portions nearer to the wall face 3 are always affected by high PMV value for all the wind directions. The average variation of PMV value nearer to the face 3 is 2.31 to 2.38. This variation in

PMV value and its magnitude is comparatively smaller for negative wind directions since the entrapped air is having possibility to travel along the wall face 3. But for the positive wind directions, the entrapped air was not able to travel near the wall face 3, instead of that the entrapped air was vented out immediately through the leeward side window. Hence it is identified that the portions nearer to face 3 and 2 is the least comfort zone. Rest of the zones is having the PMV value in the range of 2.28 to 2.21. This PMV value corresponds to one quadrant of the room interior only. To reduce the PMV value near to the wall face 3 and 2 and to create uniform comfort condition, the single vent was split in to double vent system. In the double vent system, the central portion of the room is having the PMV value of 2.23 for all the wind directions. This value is lesser by 0.05 in magnitude with reference to the single vent system. Also in the double vent system, the portions nearer to the wall face 2 are having the same PMV value as in the central region. This shows that the entrapped air is reaching to the extreme ends of the room interior in Z direction.

With the presence of 2nd vent, the portions nearer to wall face 3 are also experiencing lower PMV value in comparison with single vent system. This reduction in PMV value is about 0.2 in magnitude. In the double vent system, the high temperature was identified nearer to the roof in comparison with single vent system. Hence a triple vent system was designed which includes a third vent nearer to the roof. The triple vent system also reduces the PMV value as double vent system in the plane midplane. But its effectiveness in reducing the temperature and PMV was well identified nearer to the roof. From this PMV study, the average variation of PMV value for the single vent system was predicted as 2.21 to 2.4. For the double and triple vent system, the average variation of PMV value is 2.2 to 2.3. The average decrease of PMV value made by triple vent system was predicted as 0.2.

CONCLUSION

In this study the effect of wind direction on thermal comfort inside the room with window opening at their adjacent walls under multiple vent system was studied. CFD technique was used to simulate the internal air flow pattern. Also the CFD simulation was validated with experimental test result and network model. The effect of wind direction was studied by varying the wind direction from -67.5° to 67.5° with respect to the windward side. Wind direction made greater effect on the indoor thermal comfort and air flow characteristics. From this study, the most un-comfort zone was identified as the portions nearer to the walls which is opposite to the wind ward and lee ward side. Wind direction at negative angle creates low indoor temperature and good comfort in comparison with positive angles. In order to make the room with uniform comfort, conventional pattern of single opening in the windward side wall was changed to double and triple vent system in the same windward side wall. Performance of double and triple vent system on the indoor thermal comfort was studied for the wind directions from -45° to 45° . Finally, the thermal comfort index-Predicted mean vote contour are predicted and found that the triple vent system reduces the average PMV value by 0.3 and improves the average percentage of low temperature zone by 20% in comparison with conventional single window open system.

REFERENCES

Asfour, O. and M.B. Gadi, 2007. A comparison between CFD and network models for predicting wind-driven ventilation in buildings. *Build. Environ.*, 42: 4079-4085.

- Awbi, H.B., 2003. *Ventilation of Buildings*. 2nd Edn., Spon Press, London.
- Busch, J.F., 1992. A tale of two populations: Thermal comfort in air-conditioned and naturally ventilated offices in Thailand. *Energ. Build.*, 18: 235-249.
- Evalo, G. and V. Popov, 2006. Computational analysis of wind driven natural ventilation in buildings. *Energ. Build.*, 38: 491-501.
- Godish, T. and J.D. Spengler, 1996. Relationship between ventilation and indoor air quality: A review. *Indoor Air*, 6: 135-145.
- Larsen, T.S. and P. Heiselberg, 2008. Single sided natural ventilation driven by wind pressure and temperature difference. *Energ. Build.*, 40(6): 1031-1040.
- Marcello, C., S. Pascal and M. Dominique, 2011. Full scale experimental study of single sided ventilation: Analysis of stack and wind effects. *Energ. Build.*, 43(7): 1765-1777.
- Ramponi, R. and B. Blocken, 2012. CFD simulation of cross ventilation for a generic isolated building: Impact of computational parameters. *Build. Environ.*, 53: 34- 48.
- Ravikumar and D. Prakash, 2009. Analysis of thermal comfort in a office room by a varying the dimensions of the windows on adjacent walls using CFD: A case study based on numerical simulation. *Build. Simulat.*, 2(3): 187-196.
- Ravikumar and D. Prakash, 2011. Analysis of thermal comfort in a residential room with insect proof screen: A case study by numerical simulation methods. *Build. Simulat.*, 4(3): 217-225.
- Versteeg, H.K. and W. Malalasekara, 1995. *Introduction to Computational Fluid Dynamics: The Finite Volume Method*. Longman Scientific and Technical, Harlow.
- Visagavel, K. and P.S.S. Srinivasan, 2009. Analysis of single sided ventilation and cross ventilated room by varying width of the window opening using CFD. *Solar Energ.*, 83(1): 2-5.
- Xiong, S., Z. Guoqiang and B. Bjarne, 2012. Comparison of different methods for estimating ventilation rate through wind driven ventilated building. *Energ. Build.*, 54: 297-306.
- Zhen, B. and K. Shinsuke, 2011. Wind induced ventilation performance and airflow characteristics in an areaway-attached basement with a single sided opening. *Build. Environ.*, 40(6): 1031-1040.